Title

Thermodynamic and Structural Compensation in “Size-switch” Core Repacking Variants of Bacteriophage T4 Lysozyme

Journal

Journal of Molecular Biology, 259(3)

ISSN

0022-2836

Authors

Baldwin, Enoch
Xu, Jian
Hajiseyedjavadi, Omid
et al.

Publication Date

1996-06-01

DOI

10.1006/jmbi.1996.0338

Peer reviewed

J. Mol. Biol. (1996) **259**, 542–559

JMB

Thermodynamic and Structural Compensation in ''Size-switch'' Core Repacking Variants of Bacteriophage T4 Lysozyme

Enoch Baldwin, Jian Xu, Omid Hajiseyedjavadi, Walter A. Baase and Brian W. Matthews*

Institute of Molecular Biology, Howard Hughes Medical Institute and Department of Physics University of Oregon Eugene, Oregon 97403, USA

**Corresponding author*

Previous analysis of randomly generated multiple mutations within the core of bacteriophage T4 lysozyme suggested that the ''large-to-small'' substitution Leu121 to Ala (L121A) and the spatially adjacent ''small-to-large'' substitution Ala129 to Met (A129M) might be mutually compensating. To test this hypothesis, the individual variants L121A and A129M were generated, as well as the double ''size-switch'' mutant L121A/A129M. To make the interchange symmetrical, the combination of L121A with A129L to give L121A/A129L was also constructed.

The single mutations were all destabilizing. Somewhat surprisingly, the small-to-large substitutions, which increase hydrophobic stabilization but can also introduce strain, were less deleterious than the large-to-small replacements. Both Ala129 → Leu and Ala129 → Met offset the destabilization of L121A by about 50%. Also, in contrast to typical Leu → Ala core substitutions, which destabilize by 2 to 5 kcal/mol, Leu121 → Ala slightly stabilized A129L and A129M. Crystal structure analysis showed that a combination of side-chain and backbone adjustments partially accommodated changes in side-chain volume, but only to a limited degree. For example, the cavity that was created by the Leu121 to Ala replacement actually became larger in L121A/A129L.

The results demonstrate that the destabilization associated with a change in volume of one core residue can be specifically compensated by an offsetting volume change in an adjacent residue. It appears, however, that complete compensation is unlikely because it is difficult to reconstitute an equivalent set of interactions. The relatively slow evolution of core relative to surface residues appears, therefore, to be due to two factors. First, a mutation in a single core residue that results in a substantial change in size will normally lead to a significant loss in stability. Such mutations will presumably be selected against. Second, if a change in bulk does occur in a buried residue, it cannot normally be fully compensated by a mutation of an adjacent residue. Thus, the most probable response will tend to be reversion to the parent protein.

Keywords: correlated mutations; hydrophobic core; intragenic suppressor; packing mutants; coordinated substitutions

Introduction

Protein sequences accumulate successive substitutions through ''genetic'' drift (Kimura, 1985). Those that continue to evolve must balance detrimental mutations with either beneficial or compensatory ones (Serrano *et al*., 1993). Compensating second-site mutations (''allele-specific suppressors'') can restore wild-type properties by redressing defects caused by a deleterious substitution. These suppressors ''stabilize'' the original mutation by removing the pressure to back mutate, and thus represent an important, and perhaps rate-limiting step towards diversification of that

Present address: O. Hajiseyedjavadi, Department of Biochemistry, Oregon Health Sciences University, 3181 SW, Sam Jackson Park Road, Portland, OR 97201, USA.

0022–2836/96/230542–18 $18.00/0

sequence. How suppressor mutations effect this compensation can reveal how the original substitution exerted its phenotype (Poteete *et al*., 1991). Such mutant-suppressor pairs can also suggest equivalent allowed combinations of residues, which can be helpful in understanding the requirement for their function. Here, we analyze the structural basis of putative suppressor mutations which potentially compensate for substitutions that disrupt packing in the core of bacteriophage T4 lysozyme.

Stability changes caused by interior substitutions in proteins are usually due to changes in side-chain hydrophobicity and van der Waals interactions (for a review, see Baldwin & Matthews, 1994). Generally, large-to-small substitutions that reduce the size and hydrophobicity of interior side-chains, thereby creating or enlarging internal cavities, are destabilizing. While reduction in hydrophobicity contributes to destabilization, different amounts of destabilization in excess of the change in transfer energy (by up to 3 kcal/mol) have been observed for the same replacement in different contexts (Kellis *et al*., 1988; Shortle *et al*., 1990; Eriksson *et al*., 1992). This additional destabilization has been attributed to the cost of creating unfilled space (cavities) and the concomitant loss of favorable van der Waals interactions (Eriksson *et al*., 1992). Small-to-large substitutions that increase side-chain size are also often destabilizing (Sandberg & Terwilliger, 1989; Dao-pin *et al*., 1991; Hurley *et al*., 1992; Khorasanizadeh *et al*., 1993; Tsuji *et al*., 1993). In such ''overpacked'' variants, destabilization due to unfavorable steric contacts, disruptions of interactions with surrounding residues, or introduction of torsional strain are likely to exceed the favorable increase in hydrophobic stabilization (Karpusas *et al*., 1989; Eijsink *et al*., 1992). Nonetheless, some stabilizing small-to-large substitutions have been identified (Eijsink *et al*., 1992; Lim *et al*., 1992; Anderson *et al*., 1993; Ishikawa *et al*., 1993). In these cases, the large side-chains are accommodated with less strain, likely because they occupy space that is unfilled in the parent structure, correcting existing packing defects. Substitutions that change the shape of a side-chain but maintain or increase size and hydrophobicity may be either destabilizing or stabilizing. These results, taken together, suggest that ''packing'' and hydrophobicity (i.e. transfer free energy) have similar energetic contributions (Dao-pin *et al*., 1991; Wilson *et al*., 1992).

In order to predict the effects of core mutations on protein stability and structure, the interplay between packing and hydrophobicity must be understood. The problem can be approached by analysis of proteins of similar hydrophobicities and stabilities but having redistributed side-chain bulk. Identification of suppressors of deleterious packing mutations offers a means of generating such variants.

Compensating pairs have been identified as second-site variants that relieve a mutant phenotype (Poteete *et al*., 1991; Mitraki *et al*., 1991; di Rago *et al*., 1995) or by identifying coordinated substitutions within a protein family (Malcolm *et al*., 1990; Vernet *et al*., 1992). In another approach, we reasoned that multiply mutated proteins that contain known detrimental substitutions, but have near-wild-type function, would likely also include mutations that act as suppressors. If specific, such suppressors would directly correct the defects inflicted by the detrimental substitution.

A number of packing variants of T4 lysozyme were previously obtained by random mutagenesis of five sites, Leu121, Ala129, Leu133, Val149 and Phe153 (Baldwin *et al*., 1993a,b). Two triple-variant sequences contained the large-to-small substitution Leu121 → Ala. As a single mutant this replacement destabilizes the protein by 2.3 kcal/mol, but the multiple mutants were destabilized only 1.1 and 1.4 kcal/mol. The two multiple mutants contained also the small-to-large substitution Ala129 → Met. Since position 129 is adjacent to site 121 (see Figure 1), it seemed likely that Ala129 → Met was compensating the destabilizing effects of Leu121 → Ala (Figure 2(a)). We tested this idea by determining the thermodynamic stabilities and crystal structures of the individual cavity-containing and overpacked variants (i.e. L121A and A129M) as well as the combination mutant (L12IA/A129M). To further test the possibility of

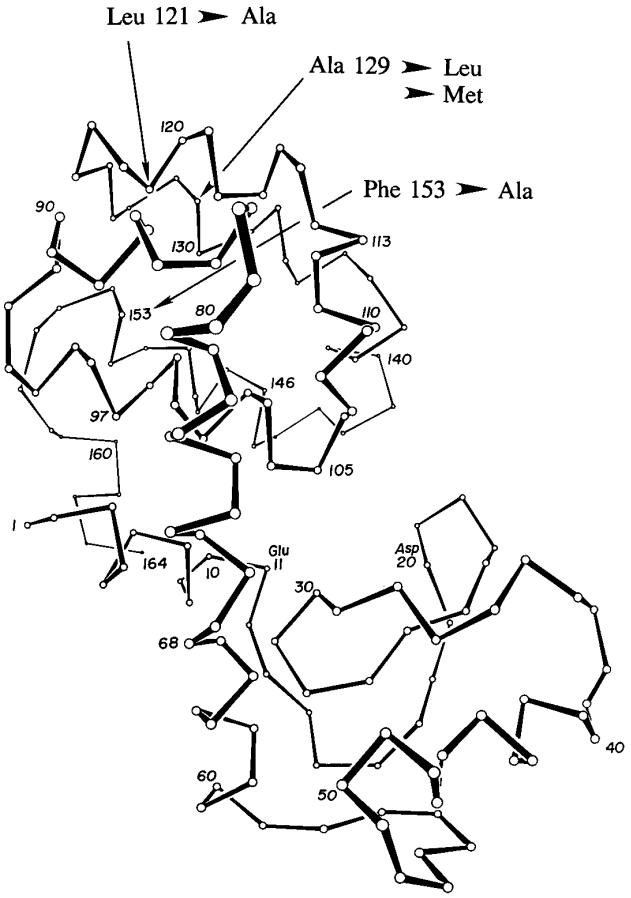

Figure 1. Schematic of the backbone of T4 lysozyme showing the locations of the substitutions discussed in the text.

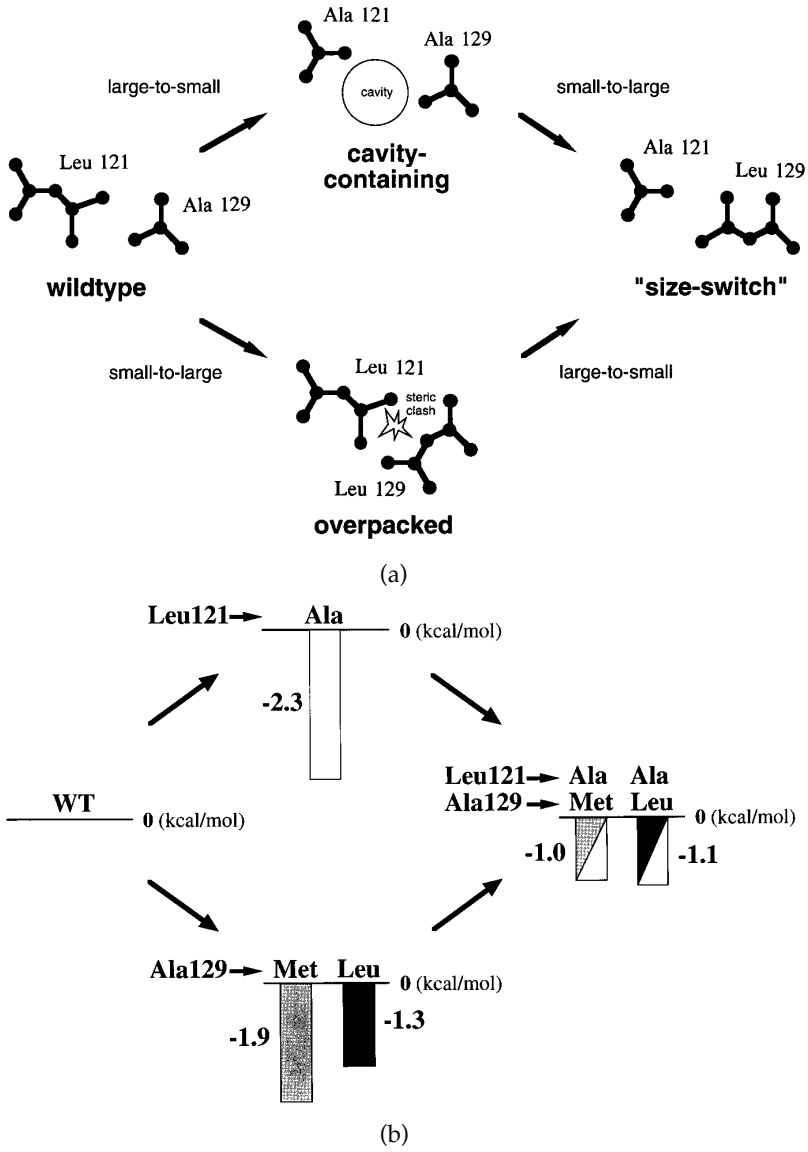

Figure 2. (a) Schematic showing how the combination of Leu121 with Ala129 is expected to be roughly equivalent to the size-switch mutant in which Leu121 is replaced by Ala and Ala129 is replaced by Leu. (b) The changes in unfolding free energy associated with the steps shown in (a). Data are also included for the combination of a methionine residue at site 129 with an alanine residue at site 121.

compensation at these two adjacent sites, and to make the interchange symmetrical, we tested the combination of L121A with A129L to give L121A/A129L. As an additional control, the double mutant A129M/F153A was made. We call the combined variants "size-switch" mutants because the residue types of the adjacent residues have been exchanged (cf. Sandberg & Terwilliger, 1989, 1991). The key question is whether compensation occurs and, related to this, whether the two side-chains can fit together well enough to preserve the local packing.

Results

The side-chains of Leu121 and Ala129 pack the interface of antiparallel helices G (residues 115 to 123) and H (residues 126 to 134: Figure 1). To test the hypothesis that A129M and L121A are compensating mutations (Figure 2(a)), we constructed the variants containing the individual substitutions. The size-switch double mutants were then made by combining L121A with A129L, and L121A with A129M. The double mutants were more stable than the cavity-containing variant L121A and were more stable than the overpacked variants A129L and A129M. On the other hand, the double mutants were not as stable as the wild-type (Figure 2(b)). This shows that there is compensation but it is not complete. The crystal structures showed that Met129 in L121A/A129M packs into the interior cavity of L121A reducing its size, while Leu129 in L121A/A129L does not. The structures and thermodynamic measurements suggest also that Leu121 → Ala reduces strain in A129M and A129L. However, the type of strain relieved in L121A/A129M is different from that in L121A/A129L. The details are given below.

Stabilities of mutant proteins

The large-to-small substitution Leu121 → Ala destabilized the wild-type protein by 2.3 kcal/mol

Table 1. Thermodynamic stabilities of variants

Mutant	t_m (°C)	Δt_m (°C)	ΔH (kcal/mol)	$\Delta\Delta G$ (kcal/mol)	$\Delta\Delta G_{nonadd}$ (kcal/mol)	$\Delta\Delta G_{tr}$ (kcal/mol)
WT*	65.3	—	132	—	—	—
L121A	59.2	–6.1	110	–2.3	—	–1.9
A129L	62.1	–3.2	112	–1.3	—	1.9
A129M	60.1	–5.2	110	–1.9	—	1.3
F153A	55.6[a]	–9.3[a]	117[a]	–3.4	—	–2.0
L121A/A129L	62.5	–2.8	118	–1.1	2.5	0.0
L121A/A129M	62.6	–2.7	121	–1.0	3.2	–0.6
A129M/F153A	52.6	–12.7	94	–4.3	1.0	–0.7

Thermal parameters for unfolding were determined by reversible thermal denaturation using circular dichroism at 223 nm to monitor helix content. t_m is the melting temperature at pH 5.4 in 0.10 M sodium chloride, 1.4 mM acetic acid, 8.6 mM sodium acetate. Δt_m is the change in t_m relative to cysteine-free wild-type (WT*). ΔH is the van't Hoff enthalpy of unfolding of the protein at its t_m. $\Delta\Delta G$ is the difference in free energies of unfolding (mutant minus wild-type) calculated at a reference temperature of 59°C using a model with a constant ΔCp of 2.5 kcal mol^{-1} deg^{-1}. For mutants where the reduction in t_m is less than 5 deg. C the estimated uncertainty in $\Delta\Delta G$ is 0.2 kcal/mol and increases to about 0.4 kcal/mol for the least stable variants. $\Delta\Delta G_{nonadd}$ is the $\Delta\Delta G$ value of the double mutant minus the sum of the $\Delta\Delta G$ values of its constituent parts. The estimated error in $\Delta\Delta G_{nonadd}$ is about 0.5 kcal/mol. $\Delta\Delta G_{tr}$ is the difference (mutant minus wild-type) in the free energies of transfer, ΔG_{tr}, from octanol to water as estimated for the replaced amino acid side-chains at 25°C using the scale given by Fauchére & Pliška (1983).

[a] From Eriksson *et al*. (1993) in 0.2 M KCl at pH 5.7. In this buffer t_m for WT* is 64.9°C and ΔH is 133 kcal/mol.

at pH 5.4 (Table 1 and Figure 2(b)). The small-to-large substitutions Ala129 → Leu and Ala129 → Met were actually less destabilizing (1.3 kcal/mol and 1.9 kcal/mol, respectively). The size-switch double mutants L121A/A129L and L121A/A129M were destabilized 1.1 and 1.0 kcal/mol, respectively. Thus, in contrast to their destabilizing effects on the wild-type, the substitutions Ala129 → Leu and Ala129 → Met stabilized L121A by 1.2 and 1.3 kcal/mol, respectively. Similarly, the Leu121 → Ala substitution stabilized A129L and A129M by 0.2 and 0.9 kcal/mol, respectively. The double mutant proteins were 2.5 to 3.2 kcal/mol more stable than expected if the destabilizing effects of the constituent substitutions were additive (Table 1).

Unlike the effect on L121A, combining Ala129 → Met with Phe153 → Ala, another large-to-small substitution at a nearby site yielded a protein of stability less than F153A.

Crystal structures

The crystal structures were determined and refined to moderate to high resolution (Table 2). The conformations of most of the residues near the mutation sites were well defined, except where mentioned. Representative difference density maps are shown in Figure 3(a) to (c). Overall changes in relative positions of backbone atoms are shown in the C^α distance-difference plots (Figure 4(a) to (g)). The conformations of the relevant side-chains are given in Table 3.

Mutant L121A

The structure of this large-to-small variant showed sizeable changes in the positions of atoms adjacent to the substitution site (Figure 5(a) and Table 4). The region around the mutation site also became generally less ordered (Table 4).

Table 2. Crystallographic data collection and refinement statistics

Mutant	Resolution (Å)	Cell dimensions *a*, *b* (Å)	Cell dimensions *c* (Å)	Completeness of data (%)	R_{merge} (%)	R_{iso} (%)	R (%)	Δ_{bond} (Å)	Δ_{angle} (°)
L121A[a]	∞–1.95	61.0	96.0	88	3.2	21.3	17.6	0.015	2.1
A129L	10–1.9	61.0	96.7	83	3.0	18.8	16.1	0.012	1.8
A129M	10–2.3	61.2	96.0	88	4.6	20.4	15.5	0.014	2.0
L121A/A129L	10–2.0	61.1	96.1	84	4.1	19.1	15.8	0.013	1.9
L121A/A129M	10–1.85	60.9	96.7	88	3.0	20.0	16.3	0.014	2.0
A129M/F153A	5–2.1	61.2	95.0	87	4.2	28.5	16.3	0.015	2.0

R_{merge} gives the agreement between independently measured reflections. R_{iso} is the average difference between the structure amplitudes of the mutant and that of wild-type. R is the crystallographic residual of the refined mutant structure. Δ_{bond} and Δ_{angle} give the average deviations of the bond lengths and angles from "ideal" values (Tronrud *et al*., 1987).

[a] This determination of the structure replaces that reported by Eriksson *et al*. (1992). See additional details in Materials and Methods.

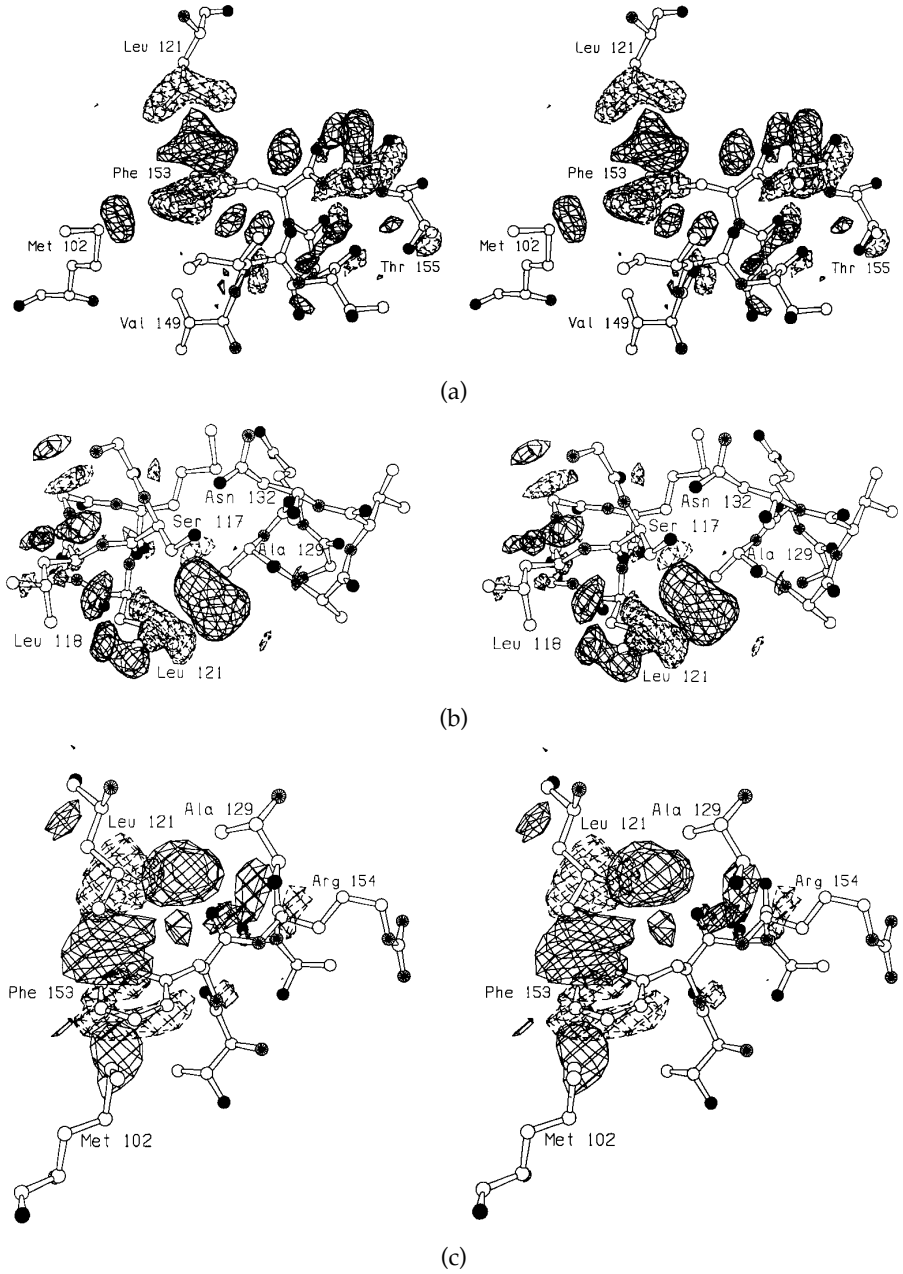

Figure 3. Difference electron density maps calculated using coefficients F_{obs}(mutant) – F_{obs}(wild-type) phased with the wild-type model. Carbon and sulfur atoms are shown as open spheres, the filled spheres represent oxygen atoms and nitrogen atoms are denoted by the partly filled spheres. Positive density is shown with continuous lines and negative density is shown with broken lines. Contours are at $\pm 4\sigma$, where σ is the rms density throughout the unit cell. (a) L121A *versus* WT; (b) A129L *versus* WT; (c) L121A/A129L *versus* WT.

The largest changes occurred in the vicinity of Phe153 (Figure 5(a)). The Phe153 side-chain changed conformation, shifting 2.4 Å towards the unfilled space created by truncation of the Leu121 side-chain, and contacting the C^{β} atom. The increase in thermal factors and the trough-like shape of the refined electron density (not shown) suggested that the Phe153 ring ''see-saws'' between two conformations, t0 and t90. The Leu118 side-chain also changed conformation from +t to an unusual '' – + '' ($\chi_1 = -104°$, $\chi_2 = 24°$) and its thermal factors increased by 19 Å^2. This rotation shifted the side-chain center-of-mass of Leu118 only 0.3 Å and modestly reduced the volume of cavity I (Table 5) by 15 Å^3.

Helix G (residues 115 to 123) rotated about its long axis (Figure 6(b)), moving the Ala121 C^{β} atom away from the interior. Other helices shifted to a smaller extent towards the interior, suggesting a ''contraction'' or ''collapse'' of the C terminus (Figure 4(a)). The overall volume of the two cavities present in the carboxy-terminal domain of the wild-type protein (Eriksson *et al.*, 1992) was increased by 21 Å^3. This is 74 Å^3 less than would

have been the case if no structural relaxation had occurred, i.e. if the Leu121 side-chain atoms had been removed and the wild-type structure retained (Table 5).

Mutant A129L

The introduced Leu129 side-chain was well ordered and occupied the most frequently observed rotamer (t–), for a leucine residue within an internal helix (Table 3). The closest contacts of the Leu129 side-chain were made with Leu121 and with Ser117 (Figure 5 (b)). The surrounding atoms shifted away from the mutant site, expanding the C-terminal domain (Figure 4(b)). The largest shift occurred in the adjacent Leu121 side-chain, which translated 1.1 Å with little torsional adjustment (Table 4), The Leu121 and Leu129 side-chains moved away from each other, increasing the distance between the C^{β} atoms by 1.0 A. Similar but smaller shifts were seen in the side-chains of Leu118 and Leu133 (0.6 and 0.7 Å rms). Phe114 translated away from the site and rotated. These shifts were primarily a consequence of rigid-body movements of helices 116-122 and 126-133, which moved them apart 0.8 Å (Figures 4(b), 6(a) and (b)). Notwithstanding the increase in bulk of the introduced side-chain, the structural changes resulted in an overall increase in the volume of the two internal cavities (Table 5).

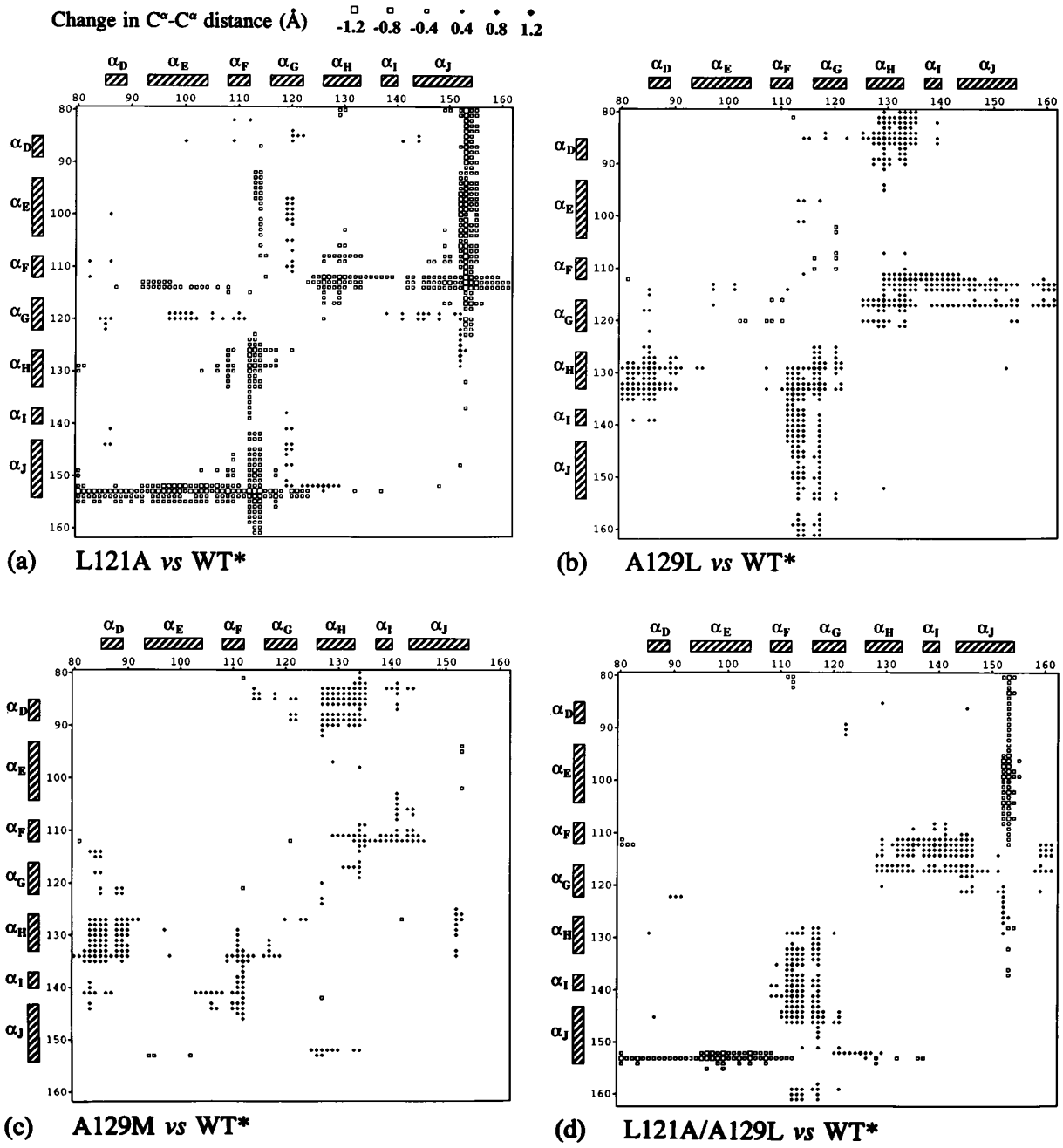

Figure 4(a–d) *legend opposite*

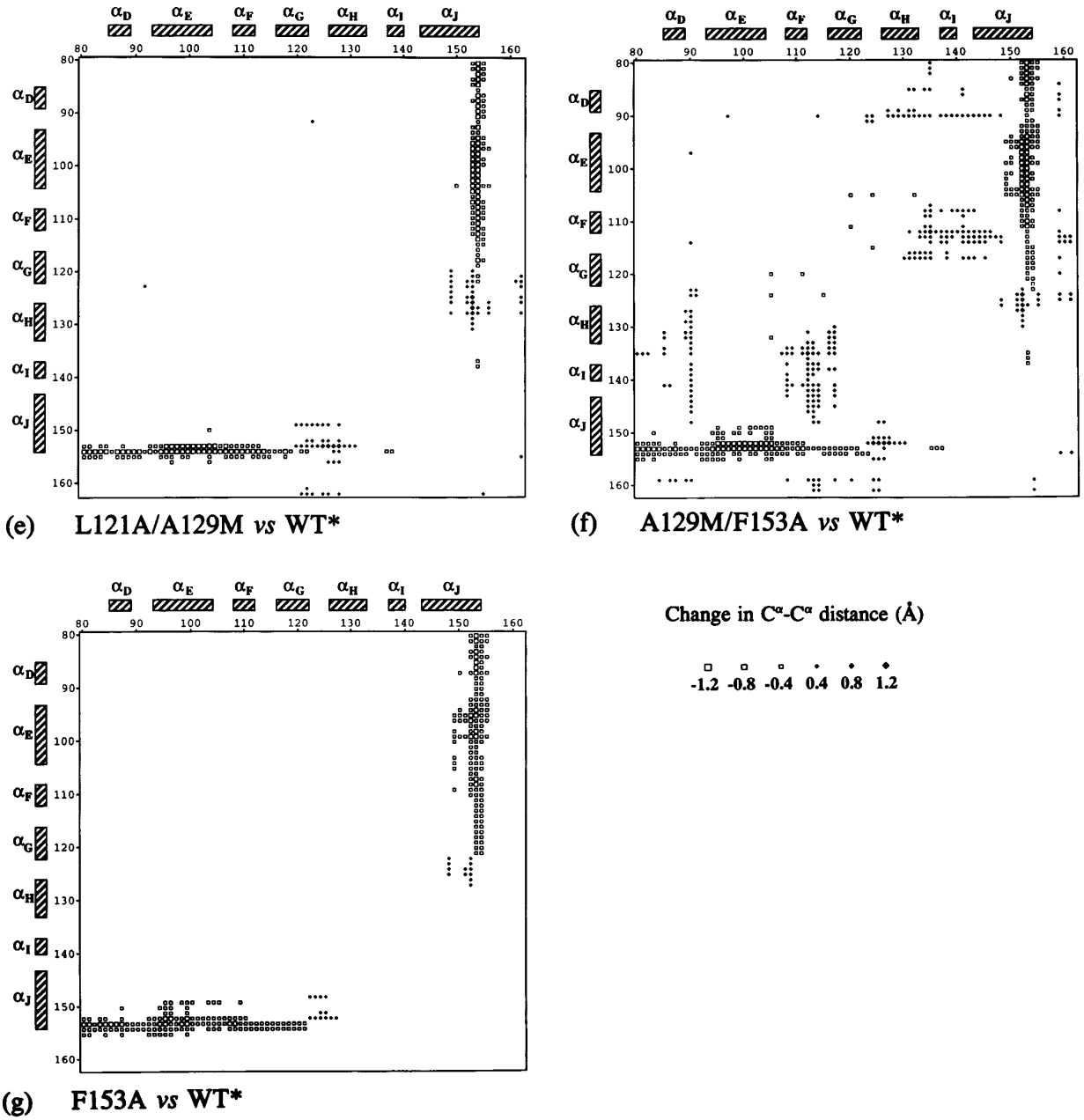

Figure 4(e–g)

Figure 4. Difference in distances between α-carbon atoms in the mutant compared to wild-type, for residues 80 to 162. The axes are the residue numbers and the change in distance between any two α-carbon atoms *i* and *j* can be found at the corresponding coordinate *i*, *j*. Pairs of atoms that moved closer in the mutant are indicated by the open squares, while those that moved apart are given by the filled diamonds. The size of the symbol is related to the magnitude of the difference and is shown in three intervals, $\geqslant 0.4$ Å, $\geqslant 0.8$ Å and $\geqslant 1.2$ Å (see the key). Pairs of α-carbon atoms in the mutant structure that remain within ± 0.4 Å of the wild-type distance are not indicated. The helices D to J include the following residues: D, 82 to 90; E, 93 to 106; F, 108 to 113; G, 115 to 123; H, 126 to 134; I, 137 to 141; and J, 143 to 155. (a) L121A *versus* WT; (b) A129L *versus* WT; (c) A129M *versus* WT; (d) L121A/A129L *versus* WT; (e) L121A/A129M *versus* WT; (f) A129M/F153A *versus* WT; (g) F153A *versus* WT.

Mutant A129M

The introduced Met129 side-chain adopted an unusual compact conformation (t– –), packing against helix 126-133 and the Leu121 side-chain (Figure 5(c) and Table 3). Met129 had higher average thermal factors than Leu129 in A129L. The closest contacts of Met129 were made with side-chains of Leu121 and Phe153, and the main-chain atoms of Trp126 and Ala130.

The largest shift occurred in the adjacent Leu121 side-chain, which rotated into a nearly eclipsed t+ conformer and had increased thermal factors. This rotation brought the Leu121 side-chain closer to the

Table 3. Torsion angles of side-chains at positions 121, 129, and 153 in the mutant structures

	Wild-type	L121A	A129L	A129M	L121A/A129L	L121A/A129M	A129M/F153A
Site 121	Leu	Ala	Leu	Leu	Ala	Ala	Leu
Rotamer	–t	–	–t	t+	–	–	t+
χ^1 (°)	289		273	228(3.1)	–	–	223(2.7)
χ^2 (°)	166		169	49	–	–	33(2.2)
Site 129	Ala	Ala	Leu	Met[a]	Leu	Met	Met[a]
Rotamer	–	–	t+	t– –	t+	tt+	t– +
χ^1 (°)			164	191	173	172	167
χ^2 (°)			70	273	59	204	254(3.6)
χ^3 (°)				317		82	91
Site 153	Phe	Phe	Phe	Phe	Phe	Phe	Ala
Rotamer	–90	t90	–90	–90	t90	t0/t90	—
χ^1 (°)	276	197	279	271	227(4.3)	219/219(4.5/3.5)	—
χ^2 (°)	129	85	130	119	134(4.5)	326/146(4.0/4.7)	—

The torsion angles are as defined by IUPAC (1970). If the deviation from the average values tabulated by Blaber *et al*. (1994) for internal helical residues exceeds two standard deviations, the number of deviations is given in parenthesis. The standard deviations for these torsion angles range from 6 to 24° and average 14°. The rotamers are as defined by Ponder & Richards (1987): 0, +, 90, t and – correspond to canonical torsion angles of 0°, 60°, 90°, 180° and 270°. Phe153 in L121A/A129M had torsion angles that were intermediate between the canonical t0 and t90 rotamers, and the deviations in standard deviations are given for both conformations.

[a] In the survey of Blaber *et al*. (1994), no t– Met residues were found at internal helical sites. The average values and standard deviations are those of the few ($n = 5$) examples that were observed at other types of sites.

Leu91 side-chain, which shifted away. As observed in the Ala129 → Leu mutant, the C-terminal domain expanded by similar but smaller backbone shifts, increasing the separation between helices G and H (Figure 4(c)). The overall cavity volume was greater than that of the wild-type and similar to A129L, but distributed differently. The small internal cavity II disappeared, the large cavity I expanded, and a new small cavity was formed between the Leu121 and Trp126 side-chains (Table 5).

Mutant L121A/A129L

The overall structure (Figure 5(d)) was a hybrid of the A129L and L121A structures, although more similar to A129L (compare Figure 4(b) and (d); and see Table 6). Helices G (115 to 123) and H (126 to 134) move apart, increasing the separation of residues 121 and 129, and expanding the C-terminal domain. The shifts were qualitatively similar to those in A129L, although the disposition of the C terminus of helix J (143 to 155) was more similar to L121A (Figure 4(a)). Residues 152 to 156 and the Phe153 side-chain shifted 0.5 Å and 1.3 Å, respectively, towards the region of the interior occupied by the Leu121 side-chain. The side-chain of Phe153 was in an unusual eclipsed conformation, unlike either wild-type or L121A (Table 3). The overall cavity volume of 100 Å^3 was among the largest for all of the mutants, primarily due to the enlargement of cavity I (Table 5). However, structural shifts did reduce the cavity volume by 52 Å^3 compared with that expected if no shift had occurred relative to the structure of A129L.

Mutant L121A/A129M

As with the L121A/A129L, the double mutant (Figure 5(e)) combined elements of the two single constituents. In contrast, however, the overall structure was more similar to L121A than to the site 129 replacement (compare Figure 4(e) with (a) and (c)); and see Table 6). The conformation of the Met129 side-chain was more extended than in A129M, reaching into the void created by the Leu121 → Ala substitution (Figure 5(e)). Met129 made closest contacts with the Ser117 and Leu121 main-chain atoms of the adjacent helix, and with the Phe153 side-chain. The Met129 side-chain thermal factors were lower than in A129M (Table 4). Phe153 rotated towards Ala121, adopting an unusual conformation intermediate between the canonical t0 and t90 rotamers.

The relative positions of helices G and H were similar to the wild-type (Figures 4(e) and 6), although they were slightly more separated. The cavity volume was the same as that of the wild-type and 90 Å^3 less than a model of A129M with Leu121 truncated (Table 5).

Mutant A129M/F153A

The overall structure was a hybrid between that of F153A and A129M and underwent substantial rearrangements in the regions of the substitutions (Figures 4(f) and 5(f)). Helices G and H rolled away from each other, separating Leu121 and Ala129, similarly to A129M. The main-chain atoms of residues 152 to 156 shifted, moving the C$^\beta$ atom of Ala153 0.9 Å deeper into the core. Similar shifts were previously observed for F153A (Eriksson *et al*., 1992, 1993; Figure 4(g)) and in L12IA (Figures 4(a) and 5(a)). The internal cavity volume increased by 56 Å^3, 80 Å^3 less than calculated for a model A129M with the 153 side-chain truncated (Table 7). The total cavity volume was smaller than in F153A (Eriksson *et al*., 1992) due to the filling in of cavity II.

Comparisons of structures

The side-chain conformations and mobility of the mutated residues depended on the context. In

L121A, A129M and A129M/F153A, accommodation of side-chain volume changes was accompanied by increased torsional strain, poorer packing and increased mobility of adjacent residues. These rearrangements propagated changes throughout the C-terminal domain. As might be expected, side-chains tended to rotate away from close contacts and towards unfilled space. In A129L, L121A/A129M and L121A/A129L, the deviations from wild-type torsion angles were less, and the unfavorable conformations observed in the other mutants were generally absent.

The conformation of the Met129 side-chain depended on the residue at position 121 (Table 3). In A129M and A129M/F153A, the methionine residue was in a compact conformation not usually observed at helical sites in general (Blaber *et al*., 1994). The side-chain atoms packed against the main-chain atoms of Trp126 and Ala130, and the Leu121 side-chain, making a number of close

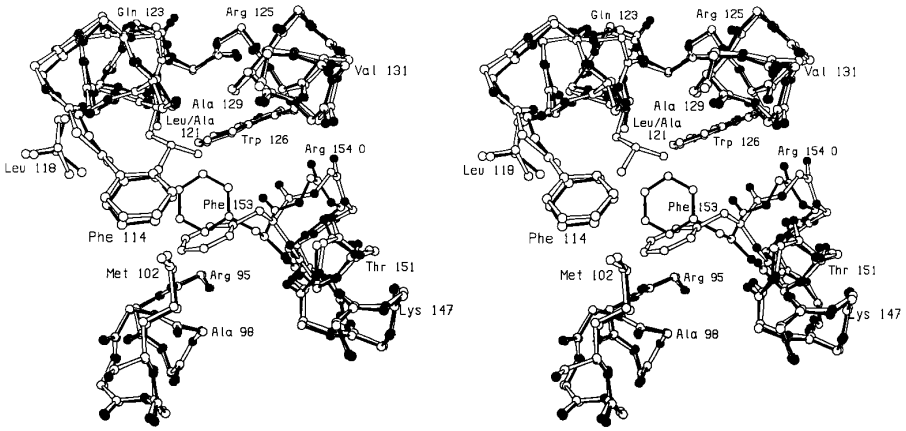

(a)

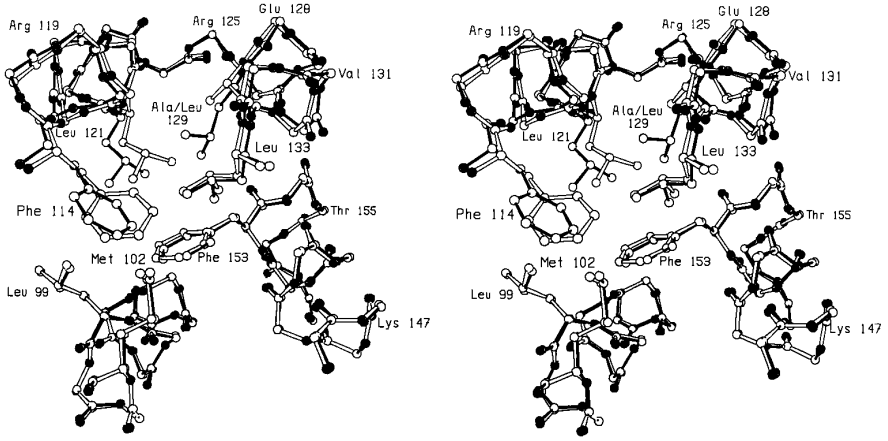

(b)

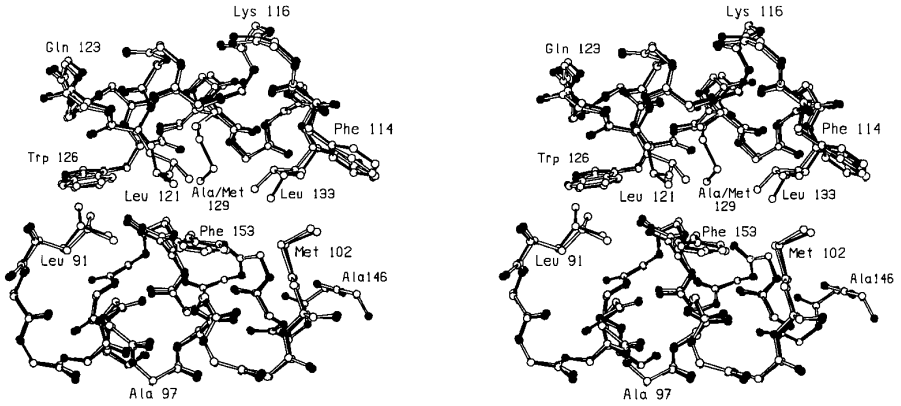

(c)

Figure 5(a–c) *legend overleaf*

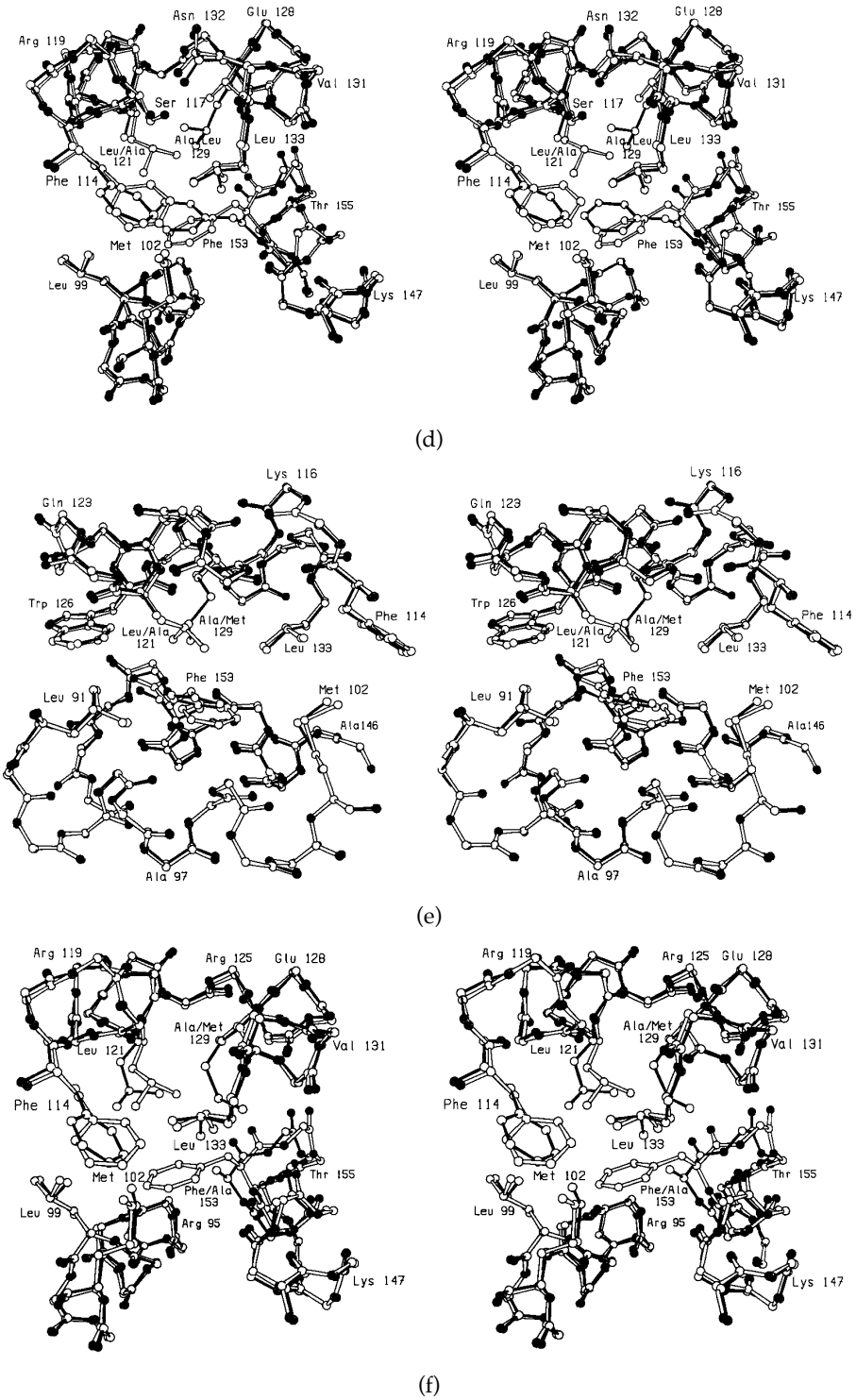

Figure 5. Comparisons of the refined models of the mutant and wild-type structures. The alignments are based on the least-squares superposition of the main-chain atoms of residues 81 to 161. Wild-type structure is shown with open bonds and the mutant structures are shown with the filled bonds. Atom types are represented as in Figure 3. (a) L121A *versus* WT; (b) A129L *versus* WT; (c) A129M *versus* WT; (d) L121A/A129L *versus* WT; (e) L121A/A129M *versus* WT; (f) A129M/F153A *versus* WT.

contacts. This conformation served to reduce the volume occupied by this side-chain.

The distance-difference plots show backbone shifts common to some variants (Figure 4(a) to (g)). Residues 152 to 157 at the C terminus of helix J shifted towards the core in variants that contained Leu121 → Ala or Phe153 → Ala (Figure 4(a) and (d) to (g)). Increased side-chain size at position 129 in A129L, A129M and A129M/F153A was accompanied by separation of helices G and H.

Table 4. Positional shifts and thermal factors of atoms near the mutation sites

Structure	Shifts in side-chain atoms (Å)[a]			Side-chain thermal factors (Å²)[b]				Atoms within 6 Å of mutation site[c]		
	Site 121	Site 129	Site 153	Site 121	Site 129	Site 153	Complete structure	No. atoms	rms shift (Å)	$\langle \Delta B \rangle$ (Å²)
WT*				18	16	18	26			
L121A	0.6	0.2	2.4 (7)	31	21	55	29	62	0.92	13
A129L	1.1 (4)	0.6	0.3 (7)	22	22	21	29	50	0.48	2
A129M	2.0 (4)	0.5	0.3 (7)	28	36	21	29	50	0.65	8
L121A/A129L	0.4	0.6	1.3 (7)	14	16	23	29	88	0.46	3
L121A/A129M	0.5	0.2	1.3 (7)	16	16	19	25	88	0.47	–1
A129M/F153A	2.1 (4)	0.1	0.9	30	37	15	32	113	0.58	5

[a] The rms shifts of side-chain atoms common to the mutant and wild-type structures. The number in parenthesis indicates the number of atoms included; otherwise the shift is that of the C^{β} atom.
[b] Average side-chain thermal factors, including C^{β} atoms.
[c] Changes in buried atoms within 6 Å of mutated side-chain(s) that are common to both structures. The atoms were selected from the WT* structure and were considered buried if their solvent-accessible surface was less than 5 Å² (Lee & Richards, 1971).

Generally, helices G and J moved the most relative to the rest of the structure (see Discussion). Interestingly, the plots for all mutants have few features corresponding to distance changes between helices D, E and F or H, I and J, suggesting that these subdomains move as two units.

As judged by the overall increase in the volume of internal cavities (Table 5), and the increased volume occupied by the buried atoms in the protein (Voronoid ''packing'' volume; Table 7), the mutants are, in general, less well packed than the wild-type. The exception is L121A/A129M, for which the packing volume decreases slightly, by an amount essentially equal to the change in van der Waals volume.

Discussion

We can begin to rationalize the changes in stability of the variants by considering the contributions of three factors: (1) solvent transfer free energy (or ''hydrophobicity''); (2) interior cavity volume; and (3) reorganization energy (or ''strain''). Changes in hydrophobicity of buried side-chains have been clearly shown to contribute to changes in protein stability (Matsumura *et al*., 1988; Kellis *et al*., 1988; Shortle *et al*., 1990; Eriksson *et al*., 1992, 1993). We use the octanol-to-water transfer energy (Fauchére & Pliška, 1983) to estimate this term. It has been shown that the formation of non-polar solvent-free cavities within a protein is destabilizing (Eriksson *et al*., 1992). We use the value of 24 cal mol^{-1} $Å^{-3}$ to estimate the destabilization associated with cavity formation (Eriksson *et al*., 1992). Any discrepancy between the hydrophobicity term plus the cavity term, and the observed change in free energy of folding, we attribute to the energy of reorganization, i.e. to strain. Table 8 summarizes the resultant analysis.

As expected, the L121A substitution is destabilizing. The small-to-large A129L and A129M substitutions are also destabilizing, although it was not

Table 5. Cavity volumes in mutant structures

Mutant	Cavity I (Å³)	Cavity II (Å³)	New cavity (Å³)	V_c (Å³)	$V_{c(mut)} - V_{c(WT*)}$ (Å³)	$V_{c(mut)} - V_{c(Ala)}$ (Å³)	V_{model} (Å³)	$V_{model} - V_c$ (Å³)
WT*[a]	33	20	—	54	—	—	—	—
L121A[a]	67	—	8[c]	75	21	—	149 (WT*)	74
A129L	56	25	—	80	26	—	—	—
A129M	69	—	9[d]	78	24	—	—	—
F153A[b]	101	32		133	79	—	156 (WT*)	23
L121A/A129L	76	24	—	100	46	25 (L12IA)	152 (A129L)	52
L121A/A129M	56	—	—	56	2	–19 (L12IA)	146 (A129M)	90
A129M/F153A	110	—	—	110	56	–22 (F153A)	190 (A129M)	80

Cavity I and cavity II are cavities in the wild-type structure as described by Eriksson *et al*. (1992). V_c is the total cavity volume as estimated using a probe radius of 1.2 Å. $V_{c(mut)} - V_{c(Ala)}$ is the change in cavity volume of double mutant (e.g. L121A/A129L) relative to the single alanine mutant given in parenthesis (e.g. L121A). V_{model} is obtained from a model calculation in which the large residue in question is truncated to alanine. In the case of L121A/A129L, for example, the ''parent'' structure used as the reference is A129L (indicated in parenthesis). In this reference structure the side-chain of Leu121 is truncated to alanine and the resulting calculated cavity volume is given as V_{model}.
[a] As discussed in Materials and Methods, mutant L121A was described by Eriksson *et al*. (1992). The data given here are from recollected data and re-refinement.
[b] From Eriksson *et al*. (1992).
[c] Cavity located between helices 93-105 and 143-154 and the side-chains of residues 153 and 150, a region occluded by Phe153 side-chain in the wild-type structure.
[d] Cavity located between the side-chains of residues 121, 126 and 129.

expected that the loss of stability would be less than for the large-to-small replacement Leu121 → Ala. In terms of the analysis in Table 8, the estimated reorganization (or strain) energy associated with the introduction of leucine or methionine is offset by the increased hydrophobicity of the replacement. Table 8 suggests that the energy of reorganization is similar for A129L and A129M (2.6 kcal/mol). The structural analysis suggests that backbone strain is more important in the first case, and side-chain strain in the latter.

In the size-switch mutant L12IA/A129L, even though there is no change in the net volume of the side-chains, the mutations result in an internal cavity that is actually larger than that in the wild-type (Table 5). When this cavity is taken into account, there is no net reorganization energy for the double mutant relative to the wild-type (Table 8). In contrast, the other size-switch mutant, L121A/A129M, results in a cavity of volume equal to that in the wild-type, but has unfavorable hydrophobicity (–0.6 kcal/mol) and reorganization terms (–0.4 kcal/mol; Table 8). In this case, the non-standard conformation of Phe153 is a potential contributor to the unfavorable reorganization energy. Thus, in both cases, the size-switch restores over half of the stability loss associated with the initial Leu121 → Ala substitution, but in neither case is the compensation perfect.

In contrast, when the sites of the large-to-small and small-to-large substitutions are further apart, as in A129M/F153A, each substitution is largely incapable of compensating for the other, and the destabilization associated with the individual substitutions is largely additive in the double mutant (Table 1). The strain energy that is introduced by the substitution A129M remains in A129M/F153A (Table 8).

The crystal structures show how shifts in the backbone and rotations of side-chains can help to accommodate volume changes due to mutations, but are also potential sources of strain of the same magnitude (cf. Karpusas *et al*., 1989). The side-chains of Leu118, Leu121, Met129 and Phe153 all adopted non-canonical conformations in at least one variant, particularly those with single substitutions. The rotations of Leu118 in L121A, and Phe153 in variants L121A, L121A/A129M and L121A/A129L towards site 121 are particularly notable. This apparent trade-off of torsional strain for cavity-filling underscores the need for allowing full side-chain conformational freedom in structure predictions.

Backbone shifts were generally associated with helix rotations and translations (as seen to a much larger degree in the evolution of the globins; Lesk & Chothia, 1980). These rigid-body adjustments included shifts of 0.33 Å in the center of mass and changes in tilt and roll angles of up to 4.5° and 5.8°, respectively (Figure 6(b)). The largest translation occurred in helix H. Helix G rotated the most, and the largest changes in tilt were seen for helices F and J, although the change for helix J is a consequence of changes in helix regularity rather than a true tilting motion (see below). The most internal helix, E, and the short helix I, which participates in a crystal contact, showed only small perturbations. At the same time there was also some

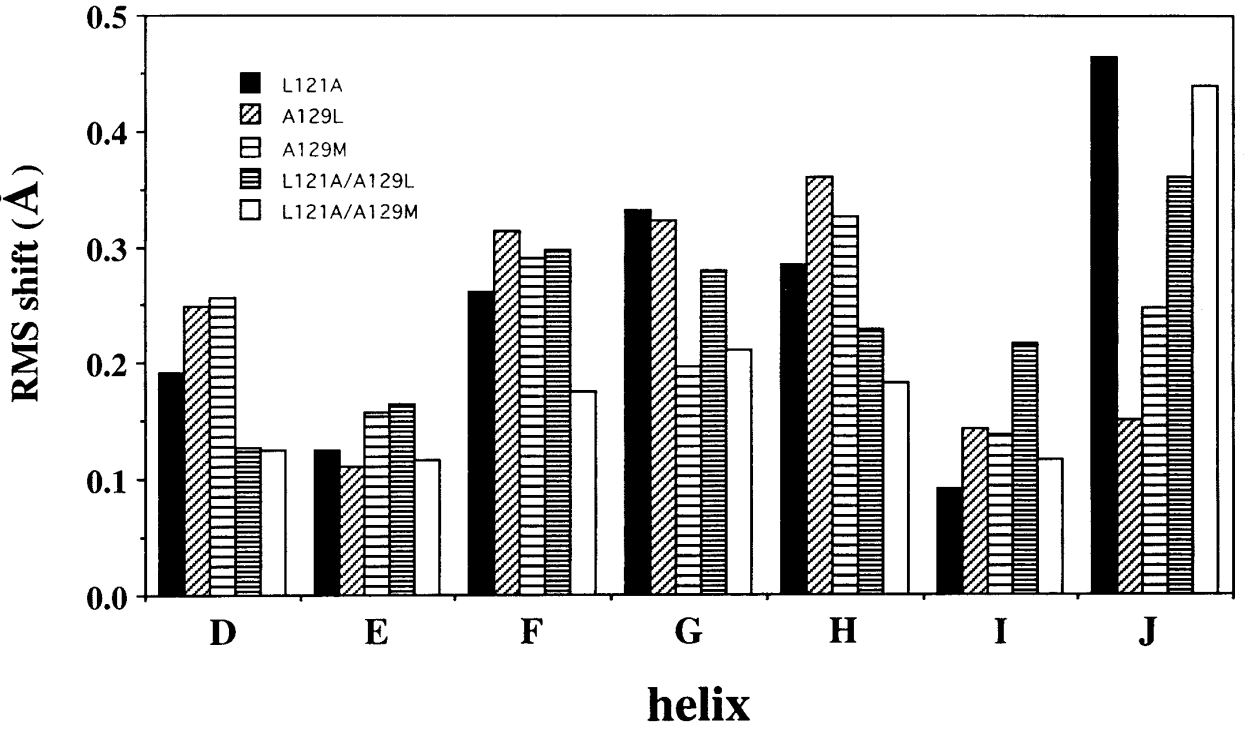

Figure 6(a) *legend overleaf*

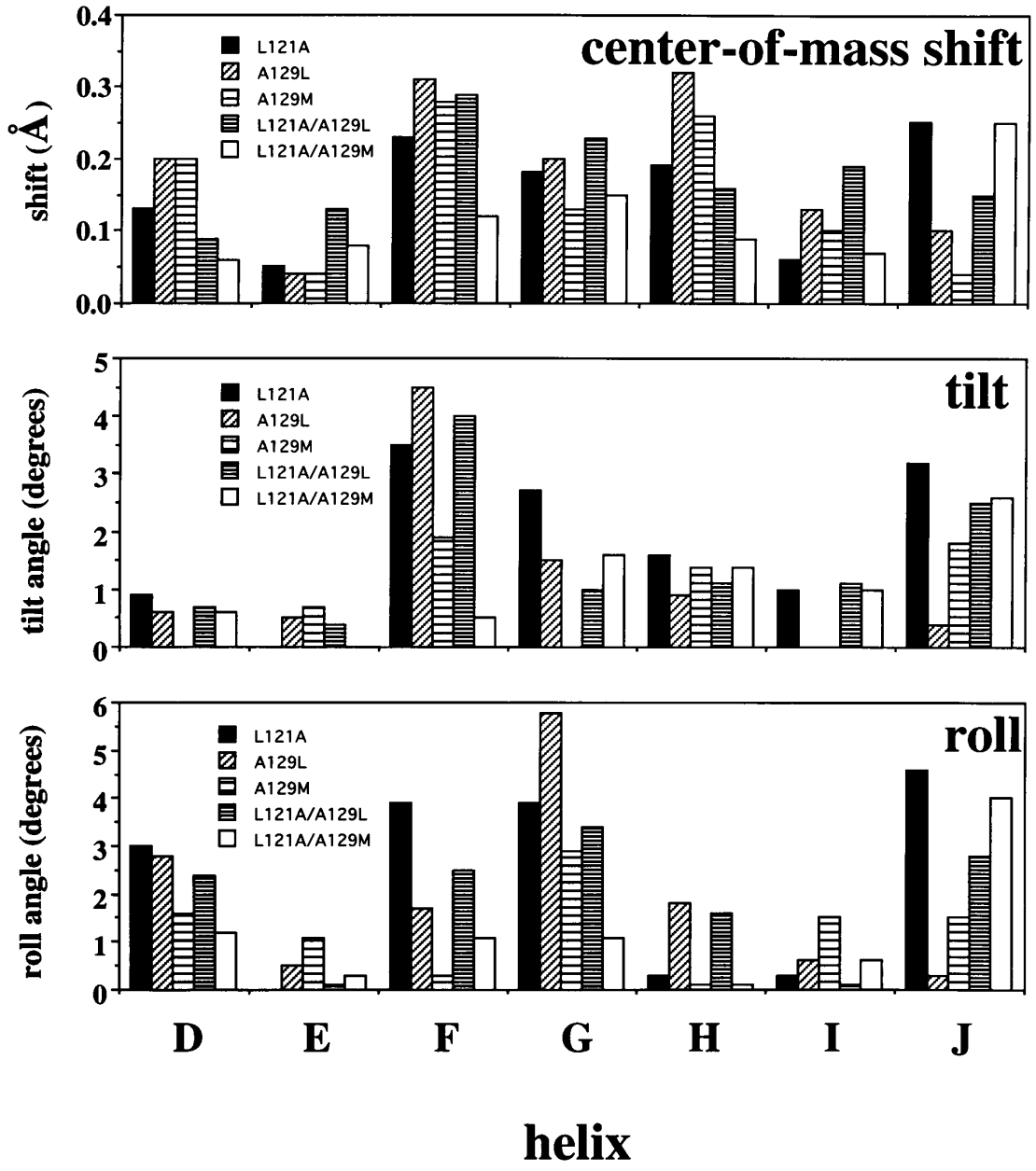

(b)

Figure 6. Rigid-body movements of helical segments relative to wild-type (see Figure 4 for identification and location of individual helices). (a) Overall rms shift; (b) dissection into center of mass shift, roll; and tilt (see the Figure). The values displayed are calculated from the transformation that superimposed a particular helical segment of the mutant onto the wild-type segment, after superposition of the main-chain atoms of the carboxy-terminal domain (residues 81 to 161). The shift is the translational component and represents the change in the average coordinate (center of mass). The roll and tilt correspond, respectively, to rotations about the helix axis and an axis perpendicular to the helix axis passing through the center of mass. The helix axis was established by first superimposing the main-chain atoms of the wild-type helix on an ideal helix aligned along a reference axis. Roll and tilt are obtained from the Eulerian angles of the rotation vector.

deformation of the individual helices themselves (Figure 7). This is not so easy to see for the main-chain atoms, for which the average shifts are of the same order of magnitude as the uncertainty in the coordinates ($\simeq 0.15$ Å; Figure 7(a)). For the C^{β} atoms, however, which are further from the axis of the helix, the distortions, up to 0.4 Å, are clearly significant (Figure 7(b)). The distortions are, in general, largest for the single mutants, and are reduced for the size-switch variants. The connection between these deformations and side-chain packing is supported by the response of helix J to alanine substitution at either Leu121 or Phe153. The resulting inward shift suggests that the wild-type helix position accommodates the contacts between these two side-chains.

Table 6. The rms discrepancies (Å) of backbone atoms within the carboxy-terminal domain (residues 81 to 161)

Mutant	Wild-type	L121A	A129L	A129M	L121A/A129L
L121A	0.30				
A129L	0.25	0.42			
A129M	0.24	0.33	0.19		
L121A/A129L	0.26	0.33	0.21	0.20	
L121A/A129M	0.23	0.18	0.20	0.27	0.22

The changes in packing volumes were localized within 6 Å of the mutation sites, since volumes calculated for atoms within 10 Å of the sites were not significantly larger (Table 7). Thus, in these variants, changing the volume of a side-chain had the greatest effect on atoms in direct contact with the altered residue.

The results suggest that the overall core volume occupied is important rather than that occupied by individual side-chains (Gerstein *et al*., 1994). Different residue combinations are able to fill similar volumes, yielding stabilities within 1 to 2 kcal/mol of that of the wild-type, but tend not to be optimal because of imperfect packing. In the size-switch variants, truncation of Leu121 removed up to 2.6 kcal/mol of strain, suggesting that interactions with this side-chain were the main source of destabilization. Stabilization equivalent to that of the wild-type is obtained only rarely, suggesting that the residue composition of the T4 lysozyme core is finely tuned. Adjustments of the backbone can partially accommodate changes in side-chain volume but only to a limited degree. This imperfect compensation is likely due to the inability of the mutant residue combinations to completely satisfy the requirements of an otherwise wild-type context. Compensation of a deleterious substitution within a close-packed protein core may be difficult, since interactions with more than one residue are likely to be affected. It is especially problematic when the surrounding contacts are primarily with main-chain atoms, which, of course, cannot be directly altered by mutation. This is exemplified by previous studies of the mutant A98V (Dao-pin *et al*., 1991). In this case, reduction in size of adjacent residues did not restore lost stability because the primary small-to-large substitution introduced unfavorable steric interactions with backbone atoms within an adjacent α-helix. In the present case, compensation may have been aided by the fact that the side-chains of residues 121 and 129 are directed toward each other (Figure 5(d)). Compensation may also have been facilitated by the presence of a pre-existing adjacent cavity in the parent structure.

The apparent difficulty in identifying perfectly compensating pairs of mutations likely explains the relatively slow evolution of protein core sequences. While the addition of further substitutions may lead to a protein as stable as the wild-type, even among substitutions of up to five residues, such combinations are apparently rare (Lim & Sauer, 1991; Baldwin *et al*., 1993a). The likelihood of sampling these during evolution depends on whether intermediate combinations are sufficiently stable to be tolerated until an equivalent arrangement is achieved. The additional constraint of optimal placement of functionally important groups may further restrict both the allowed volume changes in particular side-chains and increase the difficulty of finding compensatory substitutions (Lim *et al*., 1994).

Conclusions

The detrimental effects on thermodynamic stability from a volume change in a core residue can be, at least partially, ameliorated by a reciprocal volume change in a contacting residue. Such compensation aids in the evolutionary divergence of protein core sequences and rationalizes coordinated substi-

Table 7. Changes in van der Waals and Voronoid volumes in mutant structures

	ΔV_{vdW} (Å^3)			ΔV_{Vor} (Å^3)		$\Delta V_{Vor} - \Delta V_{vdW}$ (Å^3)	
	Extended model	6Å region	10Å region	6Å region	10Å region	6Å region	10Å region
L121A	–54	–65	–78	–53	–54	12	24
A129L	54	41	33	64	69	23	36
A129M	55	37	18	63	58	26	40
L121A/A129L	0	–8	–20	19	14	27	34
L121A/A129M	1	–6	–12	–9	–9	–3	3

Volume changes are relative to the wild-type structure. The van der Waals and Voronoid (packing) volumes (Richards, 1977) were calculated (see Materials and Methods) for all atoms within 6 Å and 10 Å of Leu121 and Leu129 in A129L, that had solvent accessibilities less than 1 Å^2 . The radii corresponded to those reported by Richards (1977). The total number of atoms included in the 6 Å and 10 Å spheres were, respectively, 90 and 227, and the Voronoid volumes for the wild-type structure were 1744 Å^3 and 3901 Å^3. For reference, the change in van der Waals volume is given for the mutant structures relative to wild-type and for a fully extended polypeptide chain. In the crystal structures, the apparent volumes are smaller, due to overlapping of the van der Waals surfaces for the radii used. In contrast, the Voronoid volumes were relatively insensitive to the particular radii set used.

Table 8. Estimation of the strain energy in the mutant structures

Mutant	Reference protein	Changes in free energy of mutant relative to reference protein: Observed value $\Delta\Delta G$ (kcal/mol)	Transfer free energy $\Delta\Delta G_{tr}$ (kcal/mol)	Cavity cost $\Delta\Delta G_{cav}$ (kcal/mol)	Inferred strain $\Delta\Delta G_{reorg}$ (kcal/mol)
L121A	Wild-type	–2.3	–1.9	–0.5	+0.1
F153A	Wild-type	–3.4	–2.0	–1.8	+0.4
A129L	Wild-type	–1.3	+1.9	–0.6	–2.6
A129M	Wild-type	–1.9	+1.2	–0.6	–2.5
L121A/A129L	Wild-type	–1.1	0	–1.1	0
	L121A	+1.2	+1.9	–0.6	–0.1
	A129L	+0.2	–1.9	–0.5	+2.6
L121A/A129M	Wild-type	–1.0	–0.6	0	–0.4
	L121A	+1.3	+1.3	+0.5	–0.5
	A129M	+0.9	–1.9	+0.5	+2.3
A129M/F153A	Wild-type	–4.3	–0.8	–1.3	–2.2
	F153A	–0.9	+1.3	+0.6	–2.8
	A129M	–2.4	–2.0	–0.8	+0.4

$\Delta\Delta G$ is the free energy of unfolding of the mutant protein relative to WT* or to the other reference protein indicated (from Table 1). $\Delta\Delta G_{tr}$ is the change in the solvent transfer free energy, also from Table 1. $\Delta\Delta G_{cav}$ is the free energy of cavity formation obtained by multiplying the increase in cavity volume in the mutant structure relative to the reference protein (Table 5) by 24 cal mol^{-1} Å^{-3}. $\Delta\Delta G_{reorg}$ is the free energy of reorganization (i.e. the strain energy), estimated as $\Delta\Delta G_{reorg} = \Delta\Delta G - \Delta\Delta G_{tr} - \Delta\Delta G_{cav}$. Note that all $\Delta\Delta G$ values refer to the free energy of unfolding so that a negative value of $\Delta\Delta G_{reorg}$ indicates the introduction of unfavorable strain energy in the mutant whereas a positive value of $\Delta\Delta G_{reorg}$ indicates the release of strain energy in the mutant relative to the reference protein.

tutions observed within some protein families (Malcolm *et al*., 1990; Vernet *et al*., 1992; Bordo *et al*., 1994; Mande *et al*., 1994) or in core repacking experiments (Lim & Sauer, 1991; Hurley *et al*., 1992; Badwin *et al*., 1993a). Based on analyses of homologous proteins, Lesk & Chothia (1980, 1982) have pointed out that compensating mutations at adjacent buried sites are rare. The relatively slow evolution of core residues relative to surface residues appears, therefore, to be due to two factors. First, a mutation in a single core residue that results in a substantial change in size will normally lead to a significant loss in stability. Such mutations will presumably be selected against. Second, if a change in bulk does occur in a buried residue, it cannot normally be fully compensated by a mutation of an adjacent residue. Thus, the most probable response will be a reversion to the parent protein.

The increased stability of size-switch relative to single variants supports the current understanding of protein stabilization. Large-to-small substitutions destabilized T4 lysozyme by reducing hydrophobicity and creating cavities. These were (partially) compensated by adjacent small-to-large substitutions that increased hydrophobicity and helped to fill voids. Destabilizing small-to-large substitutions increased hydrophobicity but also introduced strain. These, in turn, were (partially) compensated by large-to-small changes that reduced the strain. The structures illustrated that side-chain translations and rotamer switches, as well as rigid-body motions and deformations of the helix backbone are all available modes for accommodating these mutations. The strain contributions resulting from modest ($\leqslant$1.0 Å) backbone adjustments, unusual side-chain torsion angles, and steric interactions were similar in magnitude to the changes in hydrophobicity (cf. Karpusas *et al*., 1989). The myriad strategies of reorganization complicate attempts to predict structures of mutants in atomic detail. The challenge remains to understand why a particular accommodation mode is used.

Materials and Methods

Proteins

All variants were constructed in the cysteine-free wild-type lysozyme (WT*: Matsumura & Matthews, 1989). Proteins with the substitutions Leu121 → Ala (L121A) and Phe153 → Ala (F153A) have been described (Eriksson *et al*., 1992, 1993). Mutants A129M and A129L were constructed by mutagenizing an M13 clone containing the T4 lysozyme gene (Muchmore *et al*., 1989) by the method of Kunkel *et al*. (1987). The combination mutants were constructed using single-stranded M13 DNA with single mutations at site 129 as templates and the original oligonucleotide used to introduce the Leu121 → Ala mutation into wild-type. The mutant genes were cloned into the expression vector pHN1403 and expressed and purified as described (Muchmore *et al*., 1989; Poteete *et al*., 1991; Baldwin *et al*., 1993b).

Crystal growth, X-ray data collection, and refinement

Crystals in space group $P3_221$ were grown as described (Eriksson *et al*., 1993). X-ray data were collected using a Xuong-Hamlin area detector (Hamlin, 1985).

Initially, electron density maps were calculated using all of the data to the limiting resolution, with the coefficients F_o(mutant) – F_{obs}(wild-type) and $2F_o$(mutant) – F_o(wild-

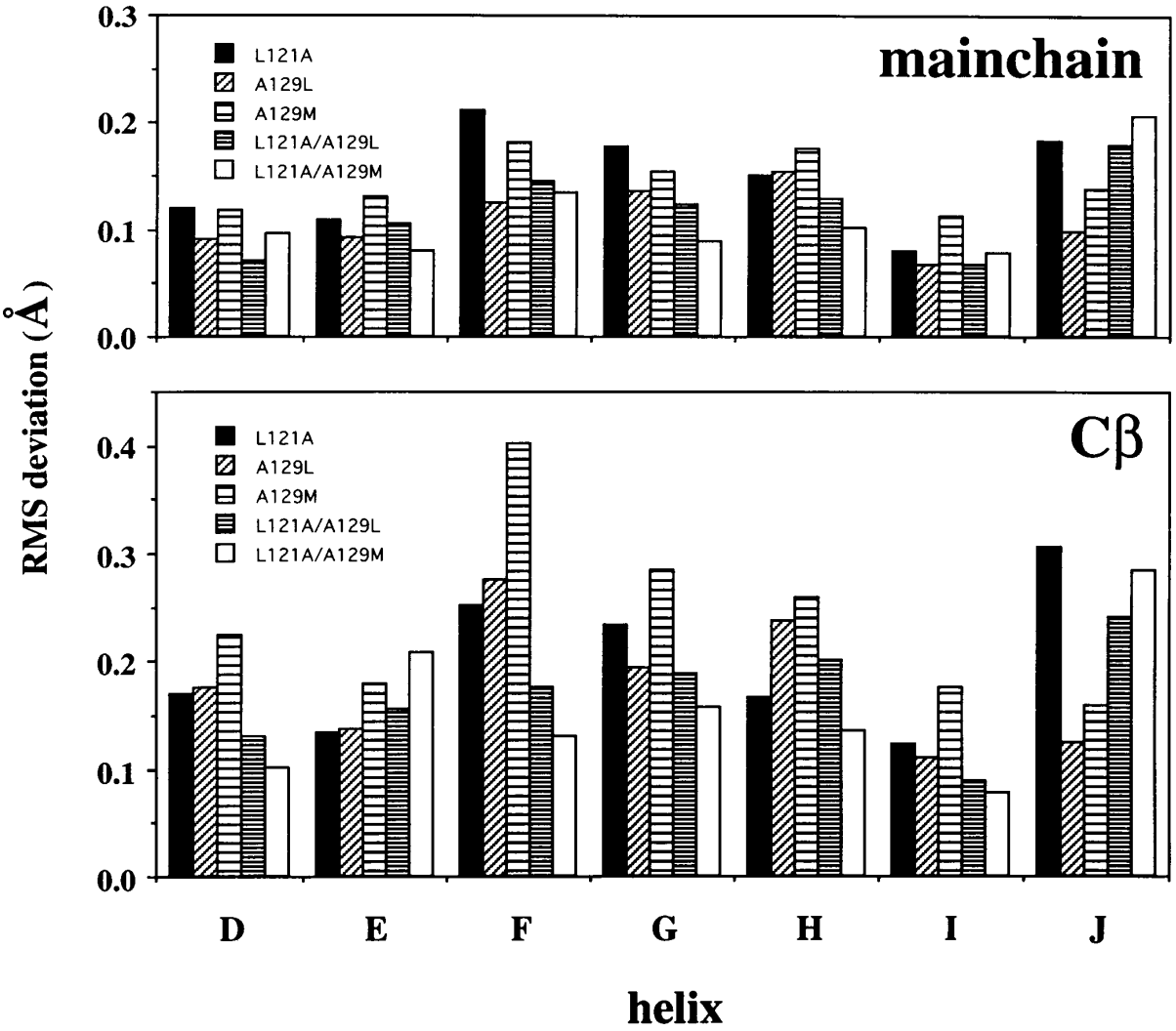

Figure 7. Deformations in the structures of individual helices in the mutant structures compared with the wild-type. (a) Deviations in main-chain atoms; (b) deviations in C^{β} atoms. These deviations were calculated after least-squares superposition of the individual helices as described in the legend to Figure 6.

type) phased with the wild-type model (Weaver & Matthews, 1987; Eriksson *et al*., 1993). These maps were used to verify the mutation and to establish the initial atom positions. Refinement was carried out using TNT (Tronrud *et al*., 1987). Rigid-body refinement first with the full model and then with it divided into five segments was performed with data between 8 Å and 4 Å resolution. If the residual remained above 0.20, further rigid-body refinement was carried out on 17 segments that define secondary structural elements using data to 3.3 Å resolution. ''Omit'' maps were used to confirm the approximate conformations of residues around the mutation site. Positional refinement was carried out first at 2.5 Å resolution and then at the limiting resolution until the *R*-factor and geometry remained constant and atomic shifts were less than 0.005 Å. Thermal factor refinement was then performed, followed by additional positional refinement. In the case of A129M (resolution 2.3 Å) the *B* values were restrained based on correlations between bonded atoms (Tronrud, 1996). Initially, the wild-type solvent molecules were included, and later adjusted by inspection. Solvent molecules with high thermal factors (>70 $Å^2$), poor electron density, or further than 3.5 Å from a hydrogen-bond donor or acceptor were removed. Additional solvent molecules were located from $F_o - F_c$ maps and added to the model where appropriate.

The X-ray structure for mutant L121A at 2.0 Å resolution has been described (Eriksson *et al*., 1992). The refinement was, however, not completely satisfactory in that the electron density for the side-chains of Leu118 and Phe153 was poorly defined. Using a new crystal, however, we have been able to collect an improved data set at 1.95 Å resolution (Table 2) and have used this to re-refine the structure. Omit, $2F_o - F_c$, and $F_o - F_c$ density maps calculated with the 1.95 Å resolution data set unambiguously indicated a new conformation for Leu118 and better defined the average conformation of Phe153. The remainder of the structure was essentially identical. For the models independently generated and refined from the 1.95 and 2.0 Å data sets, the rms discrepancy was 0.62 Å for all atoms and 0.14 Å for main-chain atoms only. The 0.62 Å value is, however, dominated by 36 atoms within highly mobile (average *B* 88 $Å^2$) side-chains that were modeled as having different rotamers in the respective refinements. If these 36 atoms are omitted the rms discrepancy for the remaining 1244 atoms is 0.25 Å.

Based on the prior refinement the increase in cavity volume resulting from the L121A mutations was 43 Å^3 (Eriksson *et al*., 1992). Based on the new refinement, the value is 21 Å^3 (Table 5). The 21 Å^3 value is actually in marginally better agreement with the energy *versus* cavity volume plot shown in Figure 2 of Eriksson *et al*. (1992) than is the previously used value of 43 Å^3. Therefore the re-refinement of L121A in no way invalidates the conclusions that were made by Eriksson *et al*. (1992). The best-fit line to the data shown in Figure 2A of Eriksson *et al*. (1992) was given as $\Delta\Delta G = a + b\Delta V$, where a = –1.9 kcal mol^{-1} and b = –0.024 kcal mol^{-1} Å^{-3}. Using the revised value of ΔV for L121A gives a = –2.1 kcal mol^{-1} and b = –0.021 kcal mol^{-1} Å^{-3}.

Coordinates of all mutants have been deposited in the Brookhaven Data Bank under accession numbers 195L-200L.

Structure comparison

Torsion angles, atomic shifts, interhelical geometry, solvent accessibility and thermal factor variations were calculated using EDPDB (Zhang & Matthews, 1995). Inter-helical separations are expressed as the distances from the center of masses of the main-chain atoms.

Cavity volumes were calculated (Connolly, 1983) using a 1.2 Å probe as described (Eriksson *et al*., 1992). Side-chain hydrophobicities were taken as the energy for transferring amino acid side-chains from octanol to water (Fauchére & Pliška, 1983).

Voronoid packing volumes as defined by Richards (1977) were calculated with a grid-based numerical algorithm (E.B., unpublished). The number of points (on a 0.1 Å grid) enclosed within the van der Waals and Voronoid volumes were counted and assigned a volume of 10^{-3} Å^3/point. A grid point was considered to be within the Voronoid volume of an atom if it was within the atom's van der Waals volume or closer to that atom's van der Waals surface than to others, essentially after Richards (1974). The same non-substituted atoms were used for all the different structures compared, and included the substituted atoms as appropriate. To minimize the effect of mobile surface side-chains on the computation, the volumes were calculated only for atoms that had less than 1 Å^3 solvent-accessible surface, as determined by EDPDB, using the method of Lee & Richards (1971) with a 1.4 Å probe.

Acknowledgements

We are most grateful to Sheila Snow and Joan Wozniak for their help in purifying and crystallizing mutant lysozymes, Larry Weaver and Dale Tronrud for advice in X-ray data collection and refinement, and Brian Shoichet and Doug Barrick for helpful comments on the manuscript. This work was supported in part by a National Institutes of Health Postdoctoral Fellowship (GM12989) to E.P.B. and a grant (GM21967) to B.W.M.

References

Anderson, D. E., Hurley, J. H., Nicholson, H., Baase, W. A. & Matthews, B. W. (1993). Hydrophobic core repacking and aromatic-aromatic interaction in the thermostable mutant of T4 lysozyme Ser117 → Phe. *Protein Sci.* **2**, 1285–1290.

Baldwin, E. P., Hajiseyedjavadi, O., Baase, W. A. & Matthews, B. W. (1993a). The role of backbone flexibility in the accommodation of variants that repack the core of T4 lysozyme. *Science*, **262**, 1715–1718.

Baldwin, E. P., Xu, J. & Hajiseyedjavadi, O. (1993b). Construction and functional selection of T4 lysozyme gene library randomized at five adjacent interior sites. In *Techniques in Protein Chemistry* (R. Angeletti, ed.), vol. 4, pp. 495–507, Academic Press, New York.

Baldwin, E. P. & Matthews, B. W. (1994). Core packing constraints, hydrophobicity and protein design. *Curr. Opin. Struct. Biol.* **5**, 396–402.

Blaber, M., Zhang, X-J., Lindstrom, J. D., Pepiot, S. D., Baase, W. A. & Matthews, B. W. (1994). Determination of α-helix propensity within the context of a folded protein: Sites 44 and 131 in bacteriophage T4 lysozyme. *J. Mol. Biol.* **235**, 600–624.

Bordo, D., Djinovic, K. & Bolognesi, M. (1994). Conserved patterns in the Cu,Zn superoxide dismutase family. *J. Mol. Biol.* **238**, 366–386.

Connolly, M. L. (1983). Solvent-accessible surfaces of proteins and nucleic acids. *Science*, **221**, 709–713.

Dao-pin, S., Alber, T., Baase, W. A., Wozniak, J. A. & Matthews, B. W. (1991). Structural and thermodynamic analysis of the packing of two α-helices in bacteriophage T4 lysozyme. *J. Mol. Biol.* **221**, 647–667.

di Rago, J. P., Herman-le Denmat, S., Paques, F., Risler, F. P., Netter, P. & Slonimski, P. P. (1995). Genetic analysis of the folded structure of yeast cytochrome *b* by selection of intragenic second-site revertants. *J. Mol. Biol.* **248**, 804–811.

Eijsink, V. G. H., Dijkstra, B. W., Vriend, G., van der Zee, J. R., Veltman, O. R., van der Vinne, B., van den Burg, B., Kempe, S. & Venema, G. (1992). The effect of cavity-filling mutations on the thermostability of Bacillus stearothermophilus neutral protease. *Protein Eng.* **5**, 421–426.

Eriksson, A. E., Baase, W. A., Zhang, X-J., Heinz, D. W., Blaber, M., Baldwin, E. P. & Matthews, B. W. (1992). The response of a protein structure to cavity-creating mutations and its relationship to the hydrophobic effect. *Science*, **255**, 178–183.

Eriksson, A. E., Baase, W. A. & Matthews, B. W. (1993). Similar hydrophobic replacements of Leu99 and Phe153 within the core of T4 lysozyme have different structural and thermodynamic consequences. *J. Mol. Biol.* **229**, 747–769.

Fauchére, J.-L. & Pliška, V. (1983). Hydrophobic parameters π of amino acid side-chains form the partioning of N-acetyl-amino-acid amides. *Eur. J. Med. Chem.* **18**, 369–375.

Gerstein, M., Sonnhammer, E. L. & Chothia, C. (1994). Volume changes in protein evolution. *J. Mol. Biol.* **36**, 1067–1078.

Hamlin, R. (1985). Multiwire area X-ray diffractometers. *Methods Enzymol.* **114**, 416–452.

Hurley, J. H., Baase, W. A. & Matthews, B. W. (1992). Design and structural analysis of alternative hydrophobic core packing arrangements in bacteriophage T4 lysozyme. *J. Mol. Biol.* **224**, 1143–1159.

International Union of Pure and Applied Chemistry-International Union of Biochemistry Commission on Biochemical Nomenclature (1970). Abbreviations and symbols for the description of the conformation of polypeptide chains. *J. Mol. Biol.* **52**, 4–17.

Ishikawa, K., Nakamura, H., Morikawa, K. & Kanaya, S. (1993). Stabilization of *Escherichia coli* ribonuclease HI by cavity-filling mutations within a hydrophobic core. *Biochemistry*, **32**, 6171–6178.

Karpusas, M., Baase, W. A., Matsumura, M. & Matthews, B. W. (1989). Hydrophobic packing in T4 lysozyme probed by cavity-filling mutants. *Proc. Natl Acad. Sci. USA*, **86**, 8237–8241.

Kellis, J. T., Nyberg, K., Sali, D. & Fersht, A. R. (1988). Contribution of hydrophobic interactions to protein stability. *Nature*, **333**, 784–786.

Khorasanizadeh, S., Peters, I. D., Butt, T. R. & Roder, H. (1993). Folding and stability of a tryptophan-containing mutant of ubiquitin. *Biochemistry*, **32**, 7054–7063.

Kimura, M. (1985). The role of compensatory neutral mutations in molecular evolution. *J. Genet.* **64**, 7–19.

Kunkel, T. A., Roberts, J. D. & Zakour, R. A. (1987). Rapid and efficient site-specific mutagenesis without phenotypic selection. *Methods Enzymol.* **154**, 367–382.

Lee, B. & Richards, F. M. (1971). The interpretation of protein structures: estimation of static accessibility. *J. Mol. Biol.* **55**, 379–400.

Lesk, A. M. & Chothia, C. (1980). How different amino acid sequences determine similar protein structures: the structure and evolutionary dynamics of the globins. *J. Mol. Biol.* **136**, 225–270.

Lesk, A. M. & Chothia, C. (1982). Evolution of proteins formed by β-sheets. II. The core of the immunoglobulin domains. *J. Mol. Biol.* **160**, 325–342.

Lim, W. A. & Sauer, R. T. (1991). The role of internal packing interactions in determining the structure and stability of a protein. *J. Mol. Biol.* **219**, 359–376.

Lim, W. A., Farruggio, D. C. & Sauer, R. T. (1992). Structural and energetic consequences of disruptive mutations in a protein core. *Biochemistry*, **31**, 4324–4333.

Lim, W. A., Hodel, A., Sauer, R. T. & Richards, F. M. (1994). Crystal structure of a mutant protein with altered but improved hydrophobic core packing. *Proc. Natl Acad. Sci. USA*, **91**, 423–427.

Malcolm, B. A., Wilson, K. P., Matthews, B. W., Kirsch, J. F. & Wilson, A. C. (1990). Ancestral lysozymes reconstructed, neutrality tested and thermostability linked to hydrocarbon packing. *Nature*, **344**, 86–89.

Mande, S., Mainfroid, M., Kalk, K. H., Goraj, K., Martial, J. A. & Hol, W. M. G. (1994). Crystal structure of triosephosphate isomerase at 2.8 Å resolution. Triosephosphate isomerase-related human genetic disorders and comparison with the trypanosomal enzyme. *Protein Sci.* **3**, 810–821.

Matsumura, M. & Matthews, B. W. (1989). Control of enzyme activity by an engineered disulfide bond. *Science*, **243**, 792–794.

Matsumura, M., Becktel, W. J. & Matthews, B. W. (1988). Hydrophobic stabilization in T4 lysozyme determined directly by multiple substitutions of Ile3. *Nature*, **334**, 406–410.

Mitraki, A., Fane, B., Haase-Pettingell, C., Sturtevant, J. & King, J. (1991). Global suppression of protein folding defects and inclusion body formation. *Science*, **253**, 54–58.

Muchmore, D. C., McIntosh, L. P., Russell, C. B., Anderson, D. E. & Dahlquist, F. W. (1989). Expression and ^{15}N labelling of proteins for proton and nitrogen-15 NMR. *Methods Enzymol.* **177**, 44–73.

Ponder, J. W. & Richards, F. M. (1987). Tertiary templates for proteins. Use of packing criteria in the enumeration of allowed sequences for different structural classes. *J. Mol. Biol.* **193**, 775–791.

Poteete, A. R., Dao-pin, S., Nicholson, H. & Matthews, B. W. (1991). Second-site revertants of an inactive T4 lysozyme mutant restore activity structuring the active site cleft. *Biochemistry*, **30**, 1425–1432.

Richards, F. M. (1974). The interpretation of protein structures: total volume, group volume distributions and packing density. *J. Mol. Biol.* **82**, 1–14.

Richards, F. M. (1977). Areas, volumes, packing and protein structure. *Annu. Rev. Biophys. Bioeng.* **6**, 151–176.

Sandberg, W. S. & Terwilliger, T. C. (1989). Influence of interior packing and hydrophobicity on the stability of a protein. *Science*, **245**, 54–57.

Sandberg, W. S. & Terwilliger, T. C. (1991). Energetics of repacking a protein interior. *Proc. Natl Acad. Sci. USA*, **88**, 1706–1710.

Serrano, L., Day, A. G. & Fersht, A. R. (1993). Step-wise mutation of barnase to binase. A procedure for engineering increased stability of proteins and an experimental analysis of the evolution of protein stability. *J. Mol. Biol.* **233**, 305–312.

Shortle, D., Stites, W. E. & Meeker, A. K. (1990). Contributions of the large hydrophobic amino acids to the stability of staphylococcal nuclease. *Biochemisty*, **29**, 8033–8041.

Tronrud, D. E. (1996). Knowledge-based temperature factor restraints for the refinement of proteins. *J. Appl. Crystallog*. In the press.

Tronrud, D. E., Ten Eyck, L. F. & Matthews, B. W. (1987). An efficient general-purpose least-squares refinement program for macromolecular structures. *Acta Crystallog. sect. A*, **43**, 489–503.

Tsuji, T., Chrunyk, B. A., Chen, X. & Matthews, C. R. (1993). Mutagenic analysis of the interior packing of an α/β barrel protein. Effects on the stabilities and rates of the α subunit of tryptophan synthase. *Biochemistry*, **32**, 5566–5575.

Vernet, T., Tessier, D. C., Khourin, H. E. & Altschuh, D. (1992). Correlation of coordinated amino acid changes at the two-domain interface of cysteine proteases with protein stability. *J. Mol. Biol.* **224**, 501–509.

Weaver, L. H. & Matthews, B. W. (1987). Structure of bacteriophage T4 lysozyme refined at 1.7 Å resolution. *J. Mol. Biol.* **193**, 189–199.

Wilson, K. P., Malcolm, B. A. & Matthews, B. W. (1992). Structural and thermodynamic analysis of compensating mutations within the core of chicken egg white lysozyme. *J. Biol. Chem.* **267**, 10842–10849.

Zhang, X-J. & Matthews, B. W. (1995). EDPDB: a multi-functional tool for protein structure analysis. *J. Appl. Crystallog.* **28**, 624–630.

Edited by P. E. Wright

(Received 25 September 1995; received in revised form 3 March 1996; accepted 18 March 1996)